

Surface modification of 3Y-TZP with cerium oxide

F.G. Marro^{*}, J. Valle, A. Mestra, M. Anglada

Dept. Ciència dels Materials i Eng. Metal., Universitat Politècnica de Catalunya, Av. Diagonal 647, 08028 Barcelona, Spain

Received 8 July 2010; received in revised form 28 September 2010; accepted 3 October 2010

Available online 1 November 2010

Abstract

Surface modification with cerium oxide of tetragonal zirconia polycrystals stabilized with 3 mol.% yttria (3Y-TZP) was carried out in order to improve the resistance to low temperature degradation. Specimens were coated with pressed CeO₂ powder and then annealed at 1400 °C and 1500 °C for periods of up to 10 h. Similar treatments were performed in specimens coated with a sub-micron CeO₂ layer by means of magnetron sputtering. Cerium penetration in the surface modified specimens is about 10 μm into the bulk and the grain size increases in the surface layer affected by cerium diffusion. The indentation bulk fracture toughness and Vickers hardness are not affected by the surface modification treatments. Berkovich nanoindentation was performed to observe the contact hardness and elastic modulus at the surface, showing no significant difference after surface modification. Surface modification with ceria induces a large increase in the resistance to hydrothermal ageing without impairing mechanical properties.

© 2010 Elsevier Ltd. All rights reserved.

Keywords: Sintering; Microstructure-final; Mechanical properties; ZrO₂; Biomedical applications

1. Introduction

Tetragonal zirconia polycrystals stabilized with 3 mol.% yttria (3Y-TZP) are being widely used in hip prosthesis and in dental restorations because of their high mechanical strength (~1000 MPa), wear resistance and excellent biocompatibility. In addition, they have moderate fracture toughness (~5 MPa m^{1/2}) which is caused by a mechanism of transformation toughening from tetragonal to monoclinic phase. The transformation takes place in the vicinity of the crack front and is accompanied by a volume increase¹ of about 4% resulting in a shielding of the crack tip as it extends. On the other hand, Kobayashi et al.² first observed in 1981 that this transformation can also initiate at the surface after ageing at low temperature in humid environments. This transformation activated by water can extend into the bulk and is accompanied by the formation of micro-cracks, resulting in a loss surface integrity and reliability after relative short times of ageing and of bulk mechanical integrity after long time exposure. Thus, TZP ceramic stabilized with yttria, ceria, calcia or magnesia is susceptible in a variable degree to degradation by water vapor and aqueous fluids.³ This phenomenon is frequently

referred to as low temperature degradation (LTD).^{3,4} In recent years, it has been shown that LTD may occur at human body temperature in the presence of body fluids in femoral heads made of 3Y-TZP. Although it may not practically change the strength after several years *in vivo*, LTD may produce roughening of the surface by phase transformation and grain pull out under contact loading. Currently, it represents a serious factor to consider for the use of 3Y-TZP in implants subjected simultaneously to contact loading and humid environment.

Since its discovery, several authors have studied different aspects of LTD degradation in TZP zirconia. The grain size plays a crucial role in determining resistance to LTD. Thus, Watanabe et al.⁵ found in 1984 that, for TZP zirconia with an yttria content between 2 and 5 mol.%, a critical grain size exists (~0.28 μm for 3 mol.% yttria) below which there was no ageing after 1000 h in air at 300 °C. Two years later, Winnubst and Burggraaf⁶ found that a 3.5 mol.% Y-TZP with a grain size of 0.1 μm was resistant to the ageing-induced phase transformation, although a 2 mol.% Y-TZP with identical grain size was susceptible to transformation. Recently, Chintapalli et al.⁷ have shown that in spark-plasma sintered 3Y-TZP zirconia with a grain size below 120 nm, no degradation occurs after 60 h autoclave exposure at 131 °C. It should be outlined here that, in order to simulate LTD degradation, frequently a pressurized vessel containing water vapor is used, since it has been reported⁸

^{*} Corresponding author. Tel.: +34 93 40 54454.

E-mail address: fernando.garcia.marro@upc.edu (F.G. Marro).

that steam sterilization at 134 °C in autoclave for 5 h simulates approximately the degradation that would take place after 15–20 years *in vivo*.

Since the stabilizer content has a strong influence on t–m transformation, changing the chemical or phase composition (both by surface modification or bulk alloying) has also been attempted to enhance LTD resistance. Nitriding of the material⁹ has been proposed to effectively enhance this resistance, but the eventual formation of a cubic phase surface layer may decrease the surface fracture toughness. Mixing with different stabilizers has also been suggested as a method to enhance hydrothermal degradation resistance.³ Thus, in 1986, Tsukuma¹⁰ observed that when stabilizing the tetragonal phase with a CeO₂ content higher than 10 mol.%, there is no monoclinic phase formation after 500 h ageing at 150 °C and 200 °C in aqueous solution. By contrast, commercially available 12Ce-TZP typically exhibits a larger grain size of 2–3 μm as compared to the usual ~0.3 μm value of 3Y-TZP, plus lower strength¹¹ (up to 800 MPa) and hardness (~7 GPa) than 3Y-TZP. Therefore, the strategy has been focused in improving the stability of the latter in front of degradation by adding small quantities of ceria, that is, in order to keep the excellent high strength of 3Y-TZP. In this context, Hernandez et al.¹² observed that by bulk alloying 3Y-TZP with more than 2 mol.% of ceria, it was prevented the formation of monoclinic phase during hydrothermal treatment at 160 °C in a pressurized vessel, while the same material without ceria showed 80% phase of monoclinic after the treatment. Along the same lines, Sato et al.¹³ concluded that uniform alloying of 3Y-TZP with more than 8 mol.% of ceria avoided phase transformation after annealing in water at 100 °C for 7 days, but the bending strength decreased by alloying from 1000 MPa (without ceria) to 300 MPa. These authors argued that such decrease in the bending strength might be due to an increase on the flaw size during the alloying process. Therefore, they proposed calcining the sintered ceramic in a ceria powder bed at 1400 °C for a period of several hours. In this way, the monoclinic content formed by ageing at 200 °C in air at 100 h was substantially reduced, while the bending strength did not decrease as much as by uniform alloying. However, it is not clear how their results on LTD in air at 200 °C may be related to the now more common tests in water vapor in autoclave at lower temperatures. Additionally, the changes in surface mechanical properties by modification with ceria were hardly studied. In the present work, the main objective is to find out whether it is possible to induce resistance to hydrothermal degradation without impairing the bulk and surface mechanical behavior of 3Y-TZP. In this sense different thermal treatments for diffusing ceria on the surface have been performed and the corresponding changes in surface mechanical properties are examined.

2. Experimental details

Commercial TZ-3YSB-E powder (Tosoh Co., Japan) was cold isostatically pressed at 200 MPa producing a green compact cylindrical bar. The bar was sintered in an alumina tube furnace (Hobersal ST-18) at 1450 °C during 2 h at 3 °C/min heating and cooling rates. The sintered body was cut into discs (2 mm thick,

10 mm φ), which were polished up to colloidal silica finishing, achieving an average roughness of less than 0.03 μm R_a. The final average grain size of the sintered body was 0.29 ± 0.13 μm. Final bulk density was measured by the Archimedes method, giving over 99% of the theoretical value of 6.06 g cm⁻³. For diffusing cerium into the surface of the sintered ceramic, each disc was covered with a fine layer of a 99.99% grade commercial CeO₂ powder (Metal Rare Earth Ltd.) in a stainless steel cylindrical mould. Then, a 10 kN uniaxial load was applied to the mould, in a direction perpendicular to the disc face. Three different times of 1, 5 and 10 h were chosen for the heat treatments at 1400 °C and these were labeled 1H1400, 5H1400 and 10H1400 respectively. A further treatment of 1 h at 1500 °C (1H1500) was carried out in order to study the effect of temperature on the quantity of cerium diffused. After the heat-treatments, the specimens were briefly polished with a 3 μm polymeric cloth in order to remove any remaining CeO₂ powder adhered to the discs. It was uncertain if, by following this procedure, only the ceria powder was removed, or, as well a very thin layer of disc was polished away. Therefore, a second set of specimens were considered which had been covered with a 160 nm CeO₂ layer by means of magnetron sputtering. This group of specimens was subjected to two heat treatments: 1 h at 1500 °C and 5 h at 1400 °C. These two treatments were chosen based on observation of the preliminary experiments of the specimens heat treated in a powder bed.

Energy dispersive spectroscopy (EDS) was used to semi-quantitatively measure the weight concentration of cerium on the surfaces of the treated specimens. The microstructure was observed by scanning electron microscopy (SEM) in the specimens after thermal etching at 1300 °C for 1 h. To obtain grain size distributions, the observed SEM micrographs were processed with standard image analysis software. The cerium diffusion profile was measured in the polished cross-section of a 5H1400 sample by electron microprobe.

The Vickers hardness HV1 was measured with a 9.8 N load. To estimate the indentation fracture toughness K_{IC} , 294.3 N Vickers indentations were performed on the surface of the samples, inducing Palmqvist cracks, from which the indentation fracture toughness was obtained by the method of Niihara¹⁴:

$$K_{IC} = 0.025 \left(\frac{E}{H_v} \right)^{0.4} \sqrt{\frac{FH_V}{4l}} \quad (1)$$

where F is the applied load, l is the total crack length at the surface and E is the Young's modulus (typically ~220 GPa for 3Y-TZP).

The strength of the treated material was determined by the ball-on-three ball biaxial flexural test performed on an Instron 8511 machine with WC balls of 6 mm diameter and a loading rate of 20 N/s. The fracture strength was evaluated as¹⁵:

$$\sigma_{MAX} = \frac{3P(1+\nu)}{4\pi t^2} \left[2 \ln \left(\frac{R_a}{0.2t} \right) + \frac{1-\nu}{1+\nu} \left(\frac{R_a}{R} \right)^2 \right] \quad (2)$$

where P is the applied load, ν is the Poisson's ratio of the material taken here as 0.33, R and t are the disk radius and thickness respectively, and R_a is the support radius defined as the distance from the disk center to the support points.

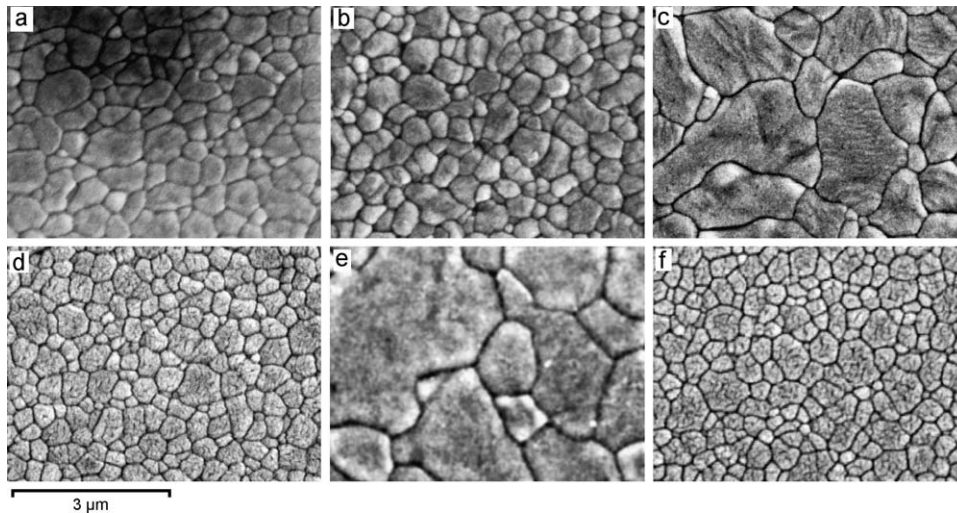


Fig. 1. SEM micrographs of 3Y-TZP specimens after being heat-treated with pressed ceria powder for different conditions: (a) 1 h at 1500 °C, (b) 1 h at 1400 °C, (c) 5 h at 1400 °C, (d) cross-section of the same sample, (e) 10 h at 1400 °C and (f) cross-section of the same sample.

Additionally, in order to analyze changes of mechanical properties in the near surface affected by diffusion, a Berkovich diamond tip was used to indent the specimens with a XP Nanoindenter (MTS) equipped with a continuous stiffness measurement (CSM) unit. The load-depth profiles were analyzed automatically to obtain the hardness and elastic modulus profiles based on the Oliver and Pharr¹⁶ method.

In order to evaluate resistance to low thermal degradation, the specimens were exposed to a 100% steam atmosphere, in an autoclave at 131 °C and 2 bar pressure for 30 h. This exposure represents a period long enough for the formation of monoclinic phase to be observable by X-rays in the as-sintered material, therefore it is ideal for evaluating the effectiveness of the treatments to enhance degradation resistance. Therefore, the present hydrothermal test simulates a degradation period at human body temperature longer than any expected implant lifetime. The accelerated degradation test was done for the surface modified samples as well as for an as-sintered specimen which served as a reference specimen in order to compare the monoclinic phase formation. X-ray diffraction was then performed with Cu K α incident radiation (1.5406 Å) in symmetric θ – 2θ configuration with a Bruker AXS D8 diffractometer. The monoclinic volume fraction was then determined by the method of Toraya et al.¹⁷:

$$V_m = \frac{1.311(I_m(\bar{1}11) + I_m(111))}{1.311(I_m(\bar{1}11) + I_m(111)) + I_t(101)} \quad (3)$$

X-ray diffraction was also performed in 2° grazing incidence configuration for the sputtered-coated specimens. This configuration was performed in an attempt to identify any remaining ceria in the surface. The mechanical integrity at the surface after hydrothermal exposure was qualitatively assessed using the scratch test (CSM Revetest) performed with a Vickers indenter at a constant load of 5 N. Finally, atomic force microscopy (AFM, Digital Instruments Multimode, tapping mode) was performed in order to assess the presence of monoclinic variants formed in the surface during hydrothermal exposure.

3. Results

Fig. 1 shows SEM images for the microstructure of 3Y-TZP material heat treated in a powder bed of CeO₂ at different times and temperatures. Table 1 shows the average grain size and cerium surface content after the treatments. As expected, the amount of cerium diffused into the ceramic increases both with the treatment duration and temperature. For 1 h at 1400 °C, the surface grains of the powder-coated surface increased slightly up to 0.37 μm as compared to the 0.29 μm original size before the treatment. Using a higher treatment temperature of 1500 °C for the same duration increases the average size of the surface grains to 0.44 μm.

The SEM images in Fig. 1(c and d) both correspond to the 1400 °C treatment during 5 h and they show, respectively, the microstructure viewed on the top surface and from a polished cross-section of the bulk. It can be seen that surface grains have grown almost to 1 μm, that is, more than twice the final size of the bulk grains, which remained below 0.5 μm. This difference between bulk and surface grains is obviously related to the higher concentration of cerium diffused in the near surface (Ce-TZP typically¹¹ exhibits a greater grain size than Y-TZP). This difference in grain size was also observed for 10H1400 (Fig. 1(e and f)). This treatment produced the largest surface grains, which had acquired a micrometric size comparable to those usually found in Ce-TZP.

Fig. 2 shows the microstructures of the sputtered-coated samples after being heat treated at (a) 1400 °C during 5 h and (b) 1500 °C during 1 h, respectively. Both treatments increase the surface grain size over 0.5 μm, but it still remains below 1 μm. However, the 5H1400 treatment produces a slight bigger increase than the 1H1500, as can be appreciated in the figure. This is also true when the heat treatments are done in powder-covered samples (Fig. 1).

After 1 h at 1400 °C, the cerium weight content detected on the surface is less than 3 wt% and it reaches 20% for the longest

Table 1
Average grain size at the surface (plus standard deviation) and surface cerium concentration for the different treatments.

Specimen	Ceria deposition method	Treatment	Grain size (μm)	Cerium (wt%)
As sintered	–	–	0.29 ± 0.13	–
1H1400	Powder bed	1400°C , 1 h	0.37 ± 0.17	2%
5H1400	Powder bed	1400°C , 5 h	0.94 ± 0.51	10%
10H1400	Powder bed	1400°C , 10 h	2.04 ± 0.37	20%
1H1500	Powder bed	1500°C , 1 h	0.44 ± 0.18	5%
Sput1H1500	Sputtering	1500°C , 1 h	0.66 ± 0.14	3%
Sput5H1400	Sputtering	1400°C , 5 h	0.78 ± 0.16	3%

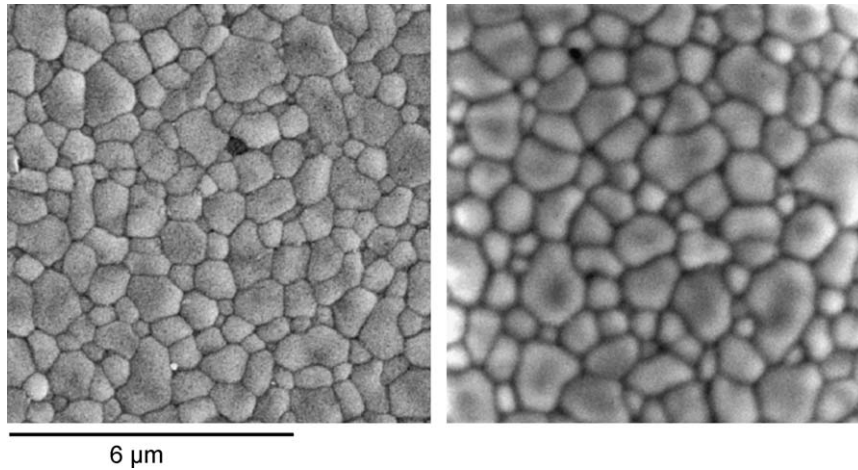


Fig. 2. SEM micrographs of 3Y-TZP specimens polished and coated with a CeO_2 thin film by magnetron sputtering. The specimens were then thermally treated at (a) 1 h at 1500°C and (b) 5 h at 1400°C .

treatment. At 1500°C for 1 h the concentration measured was 5%. On the other hand, the two treatments performed on the sputtered-coated samples only introduced a small cerium content of about 3%.

All surface modified specimens showed indentation fracture toughness similar to the original as sintered 3Y-TZP, with $K_{IC} = 5.0 \pm 0.1 \text{ MPa m}^{1/2}$. This is expected considering that the fracture toughness measured by Vickers HV30 imprints is not

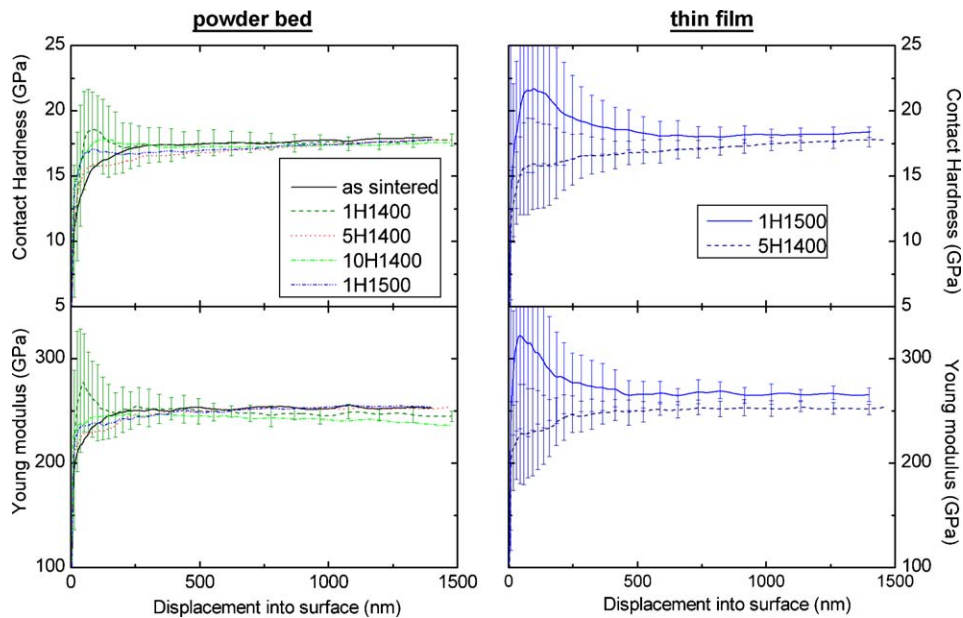


Fig. 3. Averaged nanoindentation curves showing the depth profiles of the contact hardness and elastic modulus. Calcinations in powder bed (left) and thin-film addition by sputtering (right). The data of an as-sintered specimen is shown for comparison. For the powder bed-treated specimens, the error bars of only one specimen are shown for clarity.

practically affected by the existence of the diffusion zone at the surface, since the latter is much thinner than the radius of the Palmqvist cracks considered in the K_{IC} estimation, which are about 200 μm long. That is, these cracks initiate and propagate mostly into the bulk material. The observed hardness of the treated specimens was also similar to the non-treated material, with $\text{HV1} = 11.9 \pm 0.3$ GPa, i.e. it is not affected by the presence of the surface modified layer. The strength of the treated specimens was also similar to the starting material: 1270 ± 130 MPa. Therefore, the treatments do not appear to affect the mechanical properties.

Since the depth affected by the mentioned indentation measurements is much larger than the depth affected by diffusion, Berkovich nanoindentation was performed in order to assess any change in hardness or elastic modulus in the near surface. Fig. 3 shows typical nanoindentation curves for different specimens. Each curve corresponds to the average of 10 nanoindentations per specimen. The curves are similar for the different surface modifications treatments, with a nano-Berkovich hardness of (17.0 ± 0.5) GPa and an estimated Young modulus of (245 ± 5) GPa. The curves of the sputtered-coated specimens showed a substantial error for penetration depths smaller than 0.5 μm .

Fig. 4 shows the relative cerium concentration measured on the polished cross-section of a 5H1400 specimen by electron probe microanalysis. The amount of cerium introduced falls below 90% for depths greater than 10 μm into the bulk.

Fig. 5 shows the X-ray diffraction patterns for specimens after being subjected to the hydrothermal test. At the same time, an as-sintered sample was also exposed to the water vapor to compare the formation of monoclinic phase in the non-treated material. The diffraction pattern for 1H1400 shows weaker monoclinic peaks giving a lower monoclinic content ($V_m = 58\%$) than for the degraded as sintered condition ($V_m = 69\%$). Therefore, this treatment is only effective in slightly reducing the amount of phase transformation during exposure to water. However, for all other treatments made with cerium powder, no monoclinic phase was detected after hydrothermal exposure, showing that these treatments are effective to completely avoid LTD degradation. It should be outlined here that ASTM specifications¹⁸ limit to 5% (as measured also by $K_{\alpha}\text{Cu}$ X-ray diffraction) the maximum

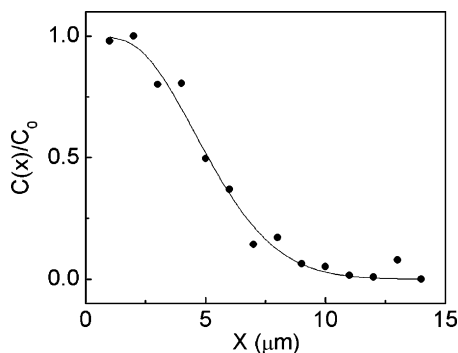


Fig. 4. Relative cerium weight concentration measured by electron probe microanalysis (EMPA) at different depths of the polished cross-section of a 5H1400 specimen.

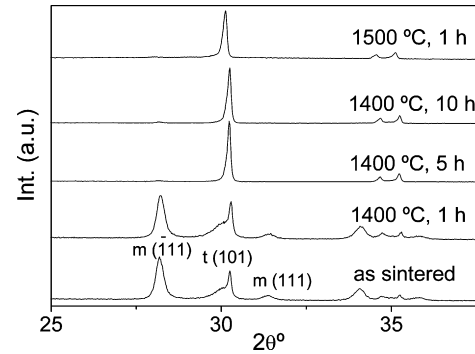


Fig. 5. X-ray diffraction patterns of as sintered and surface modified 3Y-TZP with a cerium oxide powder after being exposed to hydrothermal ageing. All spectra are normalized to the maximum peak height.

monoclinic content in a Y-TZP zirconia to be used in surgical implants.

Fig. 6 shows the X-ray diffraction patterns of Y-TZP zirconia specimens coated by CeO_2 magnetron sputtering. These patterns were obtained in a 2° grazing incidence configuration, in an effort to detect any remaining deposited ceria. The top pattern corresponds to a coated specimen without any thermal treatment and it shows the typical peaks of 3Y-TZP plus a distinct peak at $2\theta = 28.5^\circ$ corresponding to the (1 1 1) cubic plane of CeO_2 (the stronger diffracting plane of this phase), that is, to the diffraction from the deposited layer, and it disappears after the samples have been heat-treated. The two other patterns correspond to coated specimens which had been thermally treated (at 1400 $^\circ\text{C}$ for 5 h and 1500 $^\circ\text{C}$ for 1 h) and then hydrothermally aged in autoclave. It can be seen that no monoclinic phase was formed during hydrothermal exposure. This suggests that diffusing cerium from a deposited thin film can be also effective to prevent LTD in 3Y-TZP zirconia.

Fig. 7 shows the residual track of Vickers scratch performed with a constant load of 5 N on the surfaces of as sintered (AS) and of surface modified (10H1400) specimens after hydrothermal degradation. The degraded as-sintered material showed large portions of the track completely damaged. There is presence of chipping at the track borders, which had a depth of 2.5 μm and a width of about 36 μm . However, the surface-modified specimen

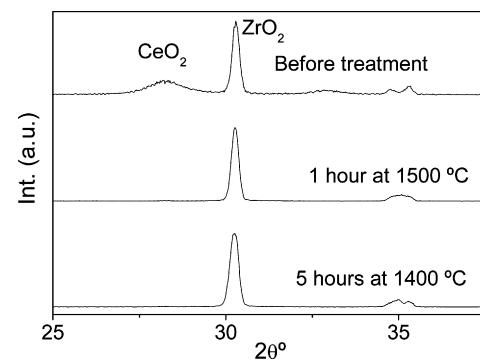


Fig. 6. 2° grazing incidence X-ray diffraction patterns of the surface modified 3Y-TZP by coating with a CeO_2 film: (top) coated sample previous to any thermal treatment, (medium) treated at 1 h 1500 $^\circ\text{C}$ and hydrothermally aged, (bottom) treated at 5 h 1400 $^\circ\text{C}$ and aged.

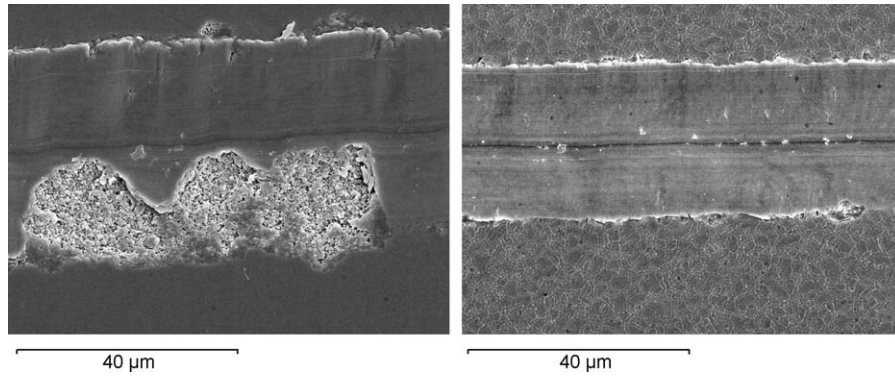


Fig. 7. SEM images showing the residual track of a Vickers scratch performed on hydrothermally exposed 3Y-TZP zirconia: as-sintered (left) and surface modified material 10H1400 (right).

showed no such severely damaged zones when performing the scratch after the autoclave exposure. Chipping is much less severe, the residual track is thinner ($28\ \mu\text{m}$) and the residual depth is only about $2\ \mu\text{m}$. This difference of behavior can be explained because, after hydrothermal exposure, the degraded layer of the as-sintered ceramic shows the presence of micro-cracking, therefore under a scratch test a higher depth will be achieved as compared to the healthy material. Therefore, these results qualitatively indicate that the mechanical properties of the surface modified zirconia are less affected by degradation.

Before degradation, the residual tracks both in the as-sintered and in the surface-modified 3Y-TZP were very similar, with equal width and depth as observed by confocal laser microscopy.

Finally, Fig. 8 shows the AFM images for the residual track after performing the scratch on the hydrothermally exposed AS and 10H1400 specimens. These images were taken at the border, because the tracks are too wide to be completely visualized by this microscopy technique. Additionally, the depth profile across the border is shown for each of the two visualized tracks. From these profiles, it can be appreciated how there is more pile-up

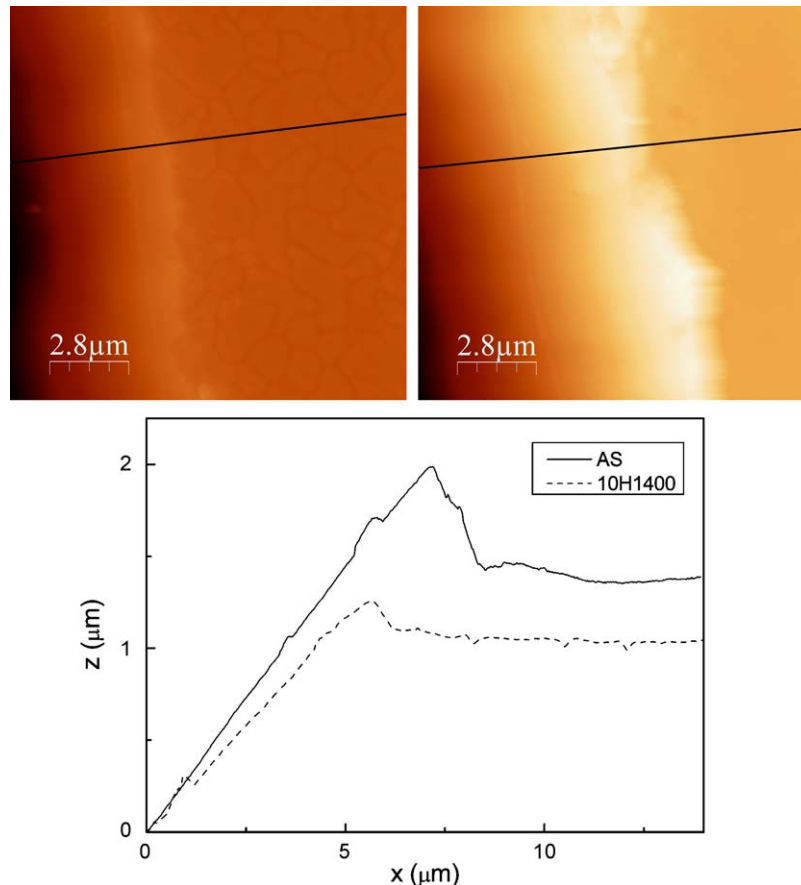


Fig. 8. AFM images of the border of the residual track produced by Vickers scratch. Scratch was performed on an AS specimen after 30 h exposure to water vapor (left) and on a 10H1400 specimen after the same exposure (right). The depth profiles of each track are represented for comparison.

of material at the track border of the hydrothermally aged AS specimen. After this aging, the surface of this specimen has transformed mainly to monoclinic and is microcracked, thus its surface shows a more plastic behavior than the 10H1400 specimen. The microstructure and phase composition of this specimen have not been affected by the aging. Therefore, there is no presence of microcracking due to a phase transformation induced by the exposure.

4. Discussion

It is well known that the number of oxygen vacancies in Y-TZP plays an important role in stabilizing the tetragonal phase.¹⁹ The increase in resistance to hydrothermal degradation observed here in the surface modified specimens should be attributed to the presence of cerium since, apparently, the only changes induced in the diffusion treatment are the introduction of cerium content at the surface together with an increase in the grain size. However, since there is overwhelming evidence that LTD resistance diminishes with a larger grain size,^{3–5} it is concluded that the effect of the cerium addition on preventing phase transformation during hydrothermal exposure is much stronger than the expected reduction in resistance to LTD induced by increasing the grain size.

It is well established that stabilizing the tetragonal phase with ceria increases the resistance to LTD, though the reason for this effect is still not clear as the tetravalent cation Ce^{4+} does not introduce vacancies. According to Li and Chen,²⁰ it seems that the tetragonal stabilization is related to the expansion of the cation lattice due to Ce^{4+} oversize with respect to Zr^{4+} and this induces oxygen vacancies to reside in lattice sites adjacent to the Zr^{4+} ion.

From all the treatments producing resistance to LTD studied here, the smallest increment in the surface grain size corresponds to the shortest duration treatments of 1 h. It is surprising that the 1H1500 treatment effectively prevents t–m transformation during LTD, since it is frequently stated¹¹ that bulk Ce-TZP needs at least 10 mol.% concentration of CeO_2 to avoid hydrothermal degradation. However, in the surface modified specimens, only about 5 wt% cerium is needed, as measured in the surface and which corresponds to about ~4 mol.% CeO_2 . As the measurements by EDX on the surface give average values on a volume of material inside a typical depth of about 1 μm , the composition concentration gradient cannot be disregarded in the near surface layer, so that the concentration in the surface grains in contact with water vapor may be significantly higher than the average concentration measured. But, the main reason to explain the resistant to LTD with this small concentration of cerium may lay in the reduced grain size, since the minimum amount of ceria (about 10 mol.%) for preventing LTD has been usually determined in bulk Ce-TZP specimens with large grain size in comparison with that achieved by surface modification. In addition the resistance to LTD in the present case is the result of the combination of the two stabilizers, CeO_2 and Y_2O_3 , which are present in the near surface region. Thus, Lin et al.²¹ produced a composition diagram showing the minimum amounts of stabilizer for TZP with different concentrations of CeO_2 and Y_2O_3 .

According to their diagram, a 3 mol.% concentration of Y_2O_3 (our base material) requires a minimum 8 mol.% concentration of CeO_2 in order to avoid degradation. However, this diagram was determined again for a larger grain size of about 1 μm ; while here the 1H1500 specimens have a final grain size below 0.5 μm . As previously said, the grain size is a critical factor in avoiding LTD; therefore a smaller grain size implies a smaller quantity of cerium required for stabilizing the tetragonal phase during hydrothermal exposure.

Ceria alloying to 3Y-TZP zirconia diminishes hardness and elastic modulus. A hardness of 8 GPa and an elastic modulus of 195 GPa have been reported²² for pure 12Ce-TZP. Therefore, one would expect to be able appreciate subtle changes by nanoindentation technique. However, it is generally believed that a nanoindentation curve correctly represents the hardness and elastic modulus of a surface layer if the penetration depth is smaller than 5% of the layer thickness. Because here the cerium penetrates upmost to a depth of about 10 μm , results of nanoindentation with penetration deeper than a few hundred nanometers will measure also invariably bulk properties, which, on the other hand, are not expected to be much different from those corresponding to the surface modified layer. Accordingly, the nanoindentation results yielded similar mechanical properties for the different conditions studied here for penetration depth larger than 200 nm. For penetration depth close to 100 nm the scatter in the measurements was too severe to deduce any feasible conclusion. In addition, the current results mainly suggest that the addition of ceria does not induce surface defects or cracks that could affect the nanoindentation elastic modulus.

5. Conclusions

- Uniaxial compaction of CeO_2 powder on 3Y-TZP and deposition of CeO_2 by magnetron sputtering followed of heat treatment near the sintering temperature, both induce a small concentration of cerium and a small increase in grain size only in a surface layer of about a few microns in thickness.
- Despite the small increase in grain size by surface modification at 1400 °C during 5 h, the formation of monoclinic phase is prevented during subsequent degradation in autoclave at 131 °C during 30 h in contact with water vapor, in contrast with the behavior of the non surface modified 3Y-TZP.
- It is possible to improve resistance to LTD in ceria surface modified 3Y-TZP without impairing excellent mechanical surface properties of 3Y-TZP.

Acknowledgements

The authors are grateful to E. Jimenez-Pique of Universitat Politècnica de Catalunya for helping in the nanoindentation tests, to D. Horwat of Institut Jean Lamour, Ecole des Mines de Nancy, for performing the magnetron sputtering experiments and to the Spanish Ministerio de Educacion for financial support under the project MAT2008-03398. J. Valle is also grateful to the Ministerio de Educacion for receiving a FP1 AP2006-00093 scholarship.

References

1. Garvie R, Hanninck RH, Pascoe RT. Ceramic steel? *Nature* 1975;**258**:703–13.
2. Kobayashi K, Kuwajima H, Masaki T. Phase change and mechanical properties of ZrO_2 - Y_2O_3 solid electrolyte after aging. *Solid State Ionics* 1981;**3-4**:489–93.
3. Lawson S. Environmental degradation of zirconia ceramics. *J Eur Ceram Soc* 1995;**15**:485–502.
4. Chevalier J, Gremillard L, Deville S. Low-temperature degradation of zirconia and implications for biomedical implants. *Annu Rev Mater Res* 2007;**37**:1–32.
5. Watanabe M, Iio S, Fukuura I. Ageing behavior in Y-TZP. Advances in ceramics. In: Claussen N, Ruhle M, Heuer AH, editors. *Science and technology of zirconia II*, vol. 12. Columbus, OH: The American Ceramic Society Inc.; 1984. p. 391–8.
6. Winnubst AJA, Burggraaf AJ. The ageing behaviour of ultrafine-grained Y-TZP in hot water. Advances in ceramics. In: Somiya S, Yamamoto N, Yanagida H, editors. *Science and technology of zirconia III*, 124. Columbus, OH: The American Ceramic Society, Inc.; 1988. p. 3948.
7. Chintapalli R, Mestra A, García Marro F, Yan H, Reece M, Anglada M. Stability of nanocrystalline spark plasma sintered 3Y-TZP. *Materials* 2010;**3**:800–14.
8. Chevalier J, Drouin JM, Cales B. Low temperature ageing behavior of zirconia hip joint heads. In: *Bioceramics: Proc. Int. Symp. Ceram. Med.*, vol. 10. 1997. p. 135–8.
9. Chung TJ, Song H, Kim GH, Kim DY. Microstructure and phase stability of yttria-doped tetragonal zirconia polycrystals heat treated in nitrogen atmosphere. *J Am Ceram Soc* 1997;**80**:2607–12.
10. Tsukuma K. Mechanical properties and thermal stability of CeO_2 containing tetragonal zirconia polycrystals. *Am Ceram Soc Bull* 1986;**65**:1386–9.
11. Tsukuma K, Shimada M. Strength, fracture toughness and Vickers hardness of CeO_2 -stabilized tetragonal ZrO_2 polycrystals. *J Mater Sci* 1985;**20**:1178–84.
12. Hernandez MT, Jurado JR, Duran P. Subeutectoid degradation of yttria-stabilized tetragonal zirconia polycrystal and ceria-doped yttria-stabilized tetragonal zirconia polycrystal ceramics. *J Am Ceram Soc* 1991;**74**:1254–8.
13. Sato T, Ohtaki, Fukushima T, Endo T, Shimada M. Mechanical properties and thermal stability of yttria-doped tetragonal zirconia polycrystals with diffused ceria in the surface. *Mater Res Soc Symp Proc* 1987;**78**:147–54.
14. Niihara K. A fracture mechanics analysis of indentation-induced Palmqvist crack in ceramics. *J Mater Sci Lett* 1983;**2**:221–3.
15. Fett T, Rizzi G, Esfehanian M, Oberacker R. Simple expressions for the evaluation of stresses in sphere-loaded disks under biaxial flexure. *J Test Eval* 2008;**36**(3):285–90. ASTM.
16. Oliver WC, Pharr GM. An improved technique for determining hardness and elastic modulus using load and displacement sensing indentation experiments. *J Mater Res* 1992;**7**:1564–83.
17. Toraya H, Yoshimura M, Somiya S. Quantitative analysis of monoclinic-stabilized cubic ZrO_2 systems by X-ray diffraction. *J Am Ceram Soc* 1984;**67**. C191-C121.
18. American Society for Testing and Materials (ASTM). *Standard specification for high-purity dense yttria tetragonal zirconium oxide polycrystal (y-tzp) for surgical implant applications*; 1873–98.
19. Guo X. Low temperature degradation mechanism of tetragonal zirconia ceramics in water: role of oxygen vacancies. *Solid State Ionics* 1998;**112**:113–6.
20. Li P, Chen I-W. Effect of dopants on zirconia stabilization – an X-ray absorption study. II. Tetravalent dopants. *J Am Ceram Soc* 1994;**77**:1281–8.
21. Lin J-D, Duh J-G, Lo C-L. Mechanical properties and resistance to hydrothermal aging of ceria- and yttria-doped tetragonal zirconia ceramics. *Mater Chem Phys* 2002;**77**:808–18.
22. Nawa M, Nakamoto S, Sekino T, Niihara K. Tough and strong Ce-TZP/alumina nanocomposites doped with titania. *Ceram Int* 1998;**24**:497–506.